Residual stress and thermal expansion behavior of TaO$_x$N$_y$ films by the micro-cantilever method

Chao-An Jong[a], Tsung-Shune Chin[a,*], Weileun Fang[b]

[a]*Department of Materials Science and Engineering, National Tsing Hua University, Hsinchu, Taiwan, ROC*
[b]*Department of Power Mechanical Engineering, National Tsing Hua University, Hsinchu, Taiwan, ROC*

Abstract

A micro-electro–mechanical system (MEMs) technique, the bilayer cantilever beam method was used to examine the residual stress and the thermal expansion coefficient (α) of TaO$_x$N$_y$ films by measuring the changes in radius of curvature. Residual stresses of all the TaO$_x$N$_y$ films RF-deposited onto SiO$_2$/Si (100) are compressive and varied from 2.5 to 12.5 MPa. The compressive stress is inversely proportional to the N$_2$/O$_2$ flow ratio except that appears at the flow ratio 0.5. However, the calculated α values, ranging from 7×10^{-7} to 2×10^{-5} °C^{-1}, increase proportionally with the N$_2$/O$_2$ flow ratio, except the value appears at the flow ratio 2. Comparing the α values of ZnS/SiO$_2$ and Si$_3$N$_4$ films, the properties of TaO$_x$N$_y$ films being optimizable by adjusting the N$_2$/O$_2$ flow ratios are obviously promising candidates in optical recording applications. Effects of other processing parameters on the α value and stress, such as the film thickness, RF power and reactive gas ratios during deposition, are also elucidated. Furthermore, a load-sensing nano-indentation method was used to examine the elastic property of the films. The obtained reduced elastic modulus E_r values of TaO$_x$N$_y$ films are nearly constant ($\sim 200 \pm 15$ GPa) at the N$_2$/O$_2$ flow ratio from 0.25 to 2. © 2001 Elsevier Science B.V. All rights reserved.

Keywords: TaO$_x$N$_y$ films; Residual stress; MEMs; Microcantilever method; Thermal expansion coefficient; Nanoindentation; Elastic modulus

1. Introduction

Because of the progress in film processing in many application fields such as electronics, magnetics and optics, the devices have been miniaturized, in an aim to achieve higher densities and speed. The thicknesses of films have actually been thinned to 50 nm or < 10 nm, as gate-oxides in complementary metal-oxide semiconductors (CMOS) or the magnetic spin-valve structure. With this step progressive miniaturization difficulty in multi-layer integration is simultaneously increased. The interaction between two nearby layers, such as diffusion and formation of interfacial compounds, desquamation may occur after some stress cycling. In order to over-come these problems it is necessary to realize the in-situ properties on sites of interest. Since these films have been usually operated under an electric, magnetic or thermal environment, the properties such as the stress state, thermal expansion behavior, hardness and elastic modulus should be well controlled. Recently, micro-electro–mechanical systems (MEMs) have caught much attention and been widely studied. By lithography, micro-scale testing structures have been made possible, not only the responses under external fields are examined but also the MEMs structure can be manipulated such as a driver for some special device application [1–4].

In this study, the mechanical properties of TaO$_x$N$_y$ were investigated. TaO$_x$N$_y$ films have been developed for a long time. For one application, oxygen was added into Ta or TaN films in order to improve the high temperature resistivity and the temperature coefficient

---

* Corresponding author. Tel.: +886-3-5742630/5711894; fax: +886-3-5719868.

E-mail address: tschin@mse.nthu.edu.tw (T.-S. Chin).

of resistivity (TCR) value of the films. The resistivity is increased proportional to the added oxygen content, so as the TCR value [5]. Due to their excellent performance in thermal insulation, the TaO_xN_y films were patented for application as heat isolating layer of magnetic optical recording media [6,7]. Yet the related behaviors are not clear in published literature. Therefore, we applied a MEMs technique, the cantilever beam method, to examine the residual stress state at room temperature and the thermal expansion coefficient by heating the sample up to 100°C. In addition, a sensing load-displacement nano-indentation method was adopted to determine the reduced elastic constant of interested films.

2. Experimental

According to requirements for different measurements, the SiO_2 single layer cantilever beams prepared by MEMs technique were used for residual stress and α measurements and bare silicon wafers for nano-indentation experiments.

2.1. Oxidization of substrate for cantilever beam preparation

In this study, the bi-layer cantilever beam method [8,9] was adopted to determine the residual stress and the α value. Thermally grown silicon dioxide (SiO_2) on a p-type Si (100) substrate, which was cleaned previously by dipping it into diluted HF and acetone and then rinsed in distilled water. After spin-drying and baked at 150°C for 30 min, the wafers were oxidized in a conventional furnace at 1050°C for a period of 160 min by a dry oxygen method. After oxidation, the thickness was examined using Nanoscope (Nanometrics Nanospec/AFT) to be approximately 1.04 μm in average. Nanoscope is a useful instrument for various materials used in VLSI processing, especially for some oxides, nitrides and polysilicon films, such as the thermal-SiO_2 by oxidation, the SiO_2 by chemical vapor deposition and polysilicon by low pressure CVD. Prior to the measurement, the optical property database such as the refractive index should be established.

2.2. Cantilever beam formation

In order to produce micro-cantilever beams, the oxide and the silicon substrates must be patterned and etched. By way of lithography, the oxides were patterned into some testing structures and due to the etching selectivity between silicon and oxide, the silicon under-layer was etched using 15 wt.% KOH solutions at 80–85°C for 30 min. Microbeams were formed with different lengths at a width of 10 μm, for instance a beam with 100 μm

(length)×10 μm (width) was used for the observation of interfering fringes and the measurement was made.

2.3. Thin film deposition

The 50-nm TaO_xN_y films were deposited by radio-frequency (RF) magnetron sputtering under an atmosphere of mixed Ar, oxygen and nitrogen. The flow ratio $(N_2 + O_2)/Ar$ was fixed at 0.1, while the flow ratio N_2/O_2 (R) was varied as 4, 2, 1. 0.5 and 0.25, respectively. A high purity (99.5%) tantalum foil with 0.3-mm thickness was used as the target. By changing the R ratio through mass flow controllers, TaO_xN_y films were prepared onto the oxide cantilever beams and bare Si (100) substrates. In the RF magnetron sputtering system, the working distance was 3 cm and the working pressure was kept at 20 mtorr.

2.4. Measurement of mechanical properties

The microbeams were bent during heating in the stage of a microscope from room temperature to 100°C that is close to the upper allowable temperature for the lens. The residual stress and the α value were obtained by measuring the radius of curvature of the deflected microcantilever beams using an optical interferometer. SEM was also used to examine the feature of the bending beam after film deposition and beam heating. The heating procedure was carried out within a chamber with a constant heating rate (1°C/min), that minimizes thermal damage, up to 100°C and the temperature deviation was kept within ±0.1°C for 2 min. The deflection of the micro-beams and the boundary rotation angle (θ) were recorded simultaneously and the schematic figure is shown in Fig. 1a. Combining with a personal computer the shifts in interference fringes due to the deformation of the beam were recorded and the change in radius of curvature can be obtained. The properties mentioned above were calculated thereof [9].

An improved nano-indentation system (Triboscope™, Hysitron) was used to measure the reduced elastic modulus (E_r) and hardness (H) of the films. The instrument continuously records both the indentation loads and displacement and from these data it is possible to derive a variety of mechanical properties. By combining with atomic force microscopy (AFM), the impression left on the sample was recorded. Here, a Berkovich diamond indenter, a triangular pyramid diamond whose depth-area relation is the same as that of a Vickers indenter, with $E_{diamond} = 1.141$ GPa and $\nu_{diamond} = 0.07$ being used. The resolutions of load and displacement were noted to be <1 nN and 0.0002 nm, respectively, according to the manufacturer.
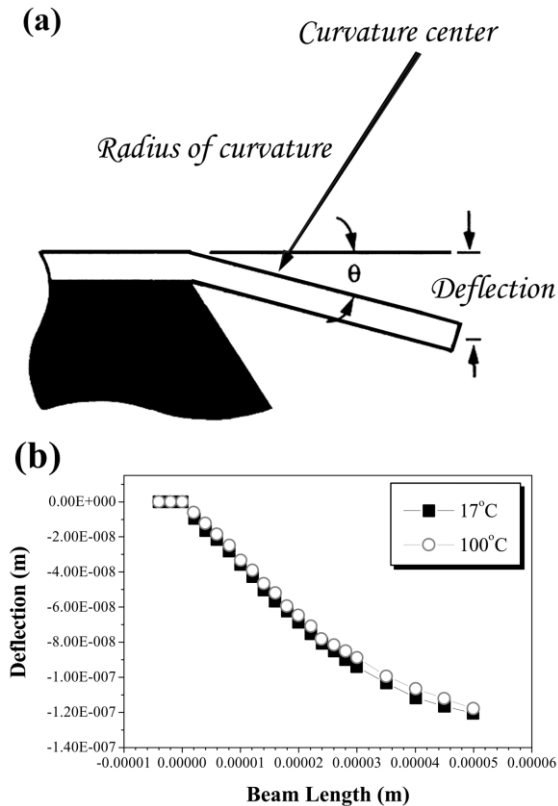
(a)

(b)

Fig. 1. (a) The schematic figure of the microcantilever beam. The measured parameters, radius of curvature of cantilever beam, deflection and relative rotation angle of beam, were shown. (b) The measured figure of single SiO_2 microcantilever obtained at 17°C (–■–) and 100°C (–○–), respectively. The measured beam length is 50 μm.

3. Results

3.1. Stress state and thermal expansion coefficient

The as-formed cantilever beams without silicon membrane curled upward naturally because of the release of residual stress. According to the measured profile of SiO_2 single layer cantilever beam, the residual stress can be calculated, and measured parameters were shown in Fig. 1a. The average residual strain of the SiO_2 beams obtained from different arrays on the same wafer was 6.8×10^{-6} and the average residual stress was 0.51 MPa where the Young's modulus was taken as 75 GPa [10]. The α value of SiO_2 beam was obtained within the temperature range of 17–100°C. After heating, the beams curled with an upward curvature as indicated with open circles in Fig. 1b. The calculated α value was 1.99×10^{-6} °C^{-1}.

Fig. 2a,b shows the feature of bending beams after film deposition as examined by SEM. After the films were deposited onto the SiO_2 substrate with a N_2/O_2 flow ratio of $R = 0.25$ and 0.5, respectively, the beams bent with a larger radius of curvature, that decreased with an elevating temperature, from 25 to 100°C. The residual stress state of the TaO_xN_y films, at $R = 0.25$ and 0.5, is compressive. Due to the α value, the SiO_2 film and TaO_xN_y film were different, the beams would bend more, curling upward during heating. That is to say, the thermal expansion of SiO_2 film is larger than that of TaO_xN_y films. The conclusions highly agree with the data of the α values.

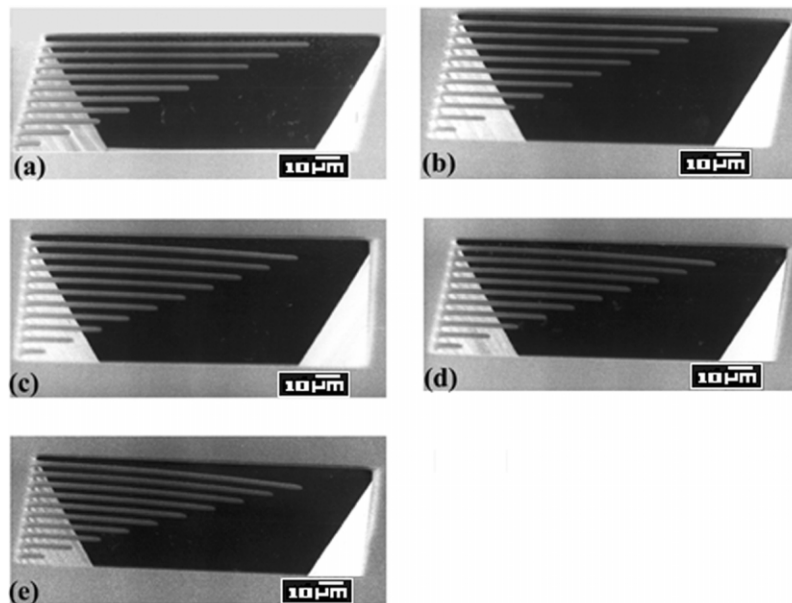At $R = 1$, the curvature of the bilayer beam changed sign from positive (upward) to negative (downward)

Fig. 2. SEM micrographs of microcantilever beams after deposition of TaO_xN_y films, (a) $N_2/O_2 = 1/4$, (b) $N_2/O_2 = 1/2$, (c) $N_2/O_2 = 1/1$, (d) $N_2/O_2 = 2$ and (e) $N_2/O_2 = 4$.
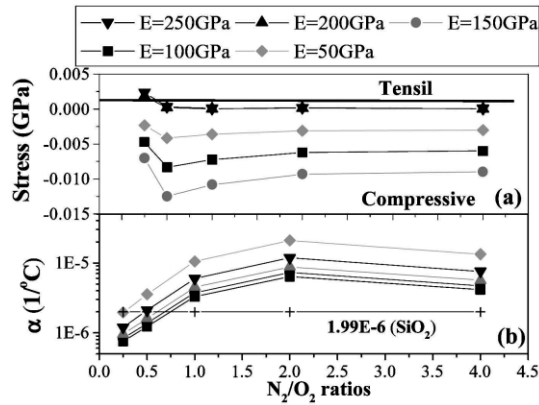
Fig. 3. The residual stress (a) and α values (b) calculated by micro-cantilever beams assuming $E_f = 50$ GPa ($\square$), $E_f = 100$ GPa ($\blacktriangledown$), $E_f = 150$ GPa ($\blacktriangle$), $E_f = 200$ GPa ($\bullet$), $E_f = 250$ GPa ($\blacksquare$).

and the beam became curled after heating from 25 to 100°C. It revealed that not only the residual stress state of the TaO$_x$N$_y$ film is compressive but also has a larger α value for TaO$_x$N$_y$ films than that of the SiO$_2$ film (Fig. 2c).

At $R = 2$ and 4, the same behavior as those films with $R = 1$ was observed. That is, the residual stress in these films is compressive and the thermal expansion is larger than that of SiO$_2$ film, (Fig. 2d,e). According to the data measured by interferometer and SEM micrographs, the residual stress and the α values are strongly affected by R ratio.

Furthermore, the bilayer cantilever will be bent during film deposition with a radius of curvature if the thermal strains of these two films are different. In this case, combining the intrinsic and thermal strains of two different films, calculations of the total strain of the bilayer beam can be simplified, according to Timoshenko [11], as following:

$$\in_{total} = \frac{\left[(r_2 - r_1) \times \dfrac{t_f}{2}\right] + (r_2 - r_1) \times \dfrac{E_B(t_f + t_B)}{2(E_f + E_B)}}{r_1 r_2 + \dfrac{r_1 t_f}{2} + r_1 \times \left[\dfrac{E_B(t_f + t_B)}{2(E_f + E_B)}\right]} \quad (1)$$

$$\in_f = \in_{total} - \in_{oxide} \quad (2)$$

Here, the E_f, t_f and E_B and t_B are the elastic constant and thickness of TaO$_x$N$_y$ film and SiO$_2$ substrate, respectively. The values r_1 and r_2 are the radius of curvature for the single and bilayer beams, respectively and both are calculated from the curvature center to the neutral axis. Thus, the residual stress, which is a function of E_f can be calculated by the formula:

$$\sigma_f = f(E_f) = E_f \in_f \quad (3)$$

Since the Young's modulus of the TaO$_x$N$_y$ film is not available, the parameter E_f is taken as arbitrary values between 50 and 250 GPa for comparison purposes. The

difference in the α value ($\Delta\alpha = \alpha_{oxide} - \alpha_f$) introduced by the temperature change (ΔT) was calculated by the relationship between the change of radius of curvature $[= \Delta(1/\rho)]$ and $\Delta\alpha$ of the bilayer beam [9]:

$$\Delta\left(\frac{1}{\rho}\right) = \frac{6 \cdot \Delta T \cdot \Delta\alpha_f \cdot (1 + m)^2}{h \cdot [3 \cdot (1 + m)^2 + (1 + m \cdot n)(m^2 + m \cdot n))]} \quad (4)$$

Where h is the total thickness of bilayer beam ($= h_{oxide} + h_f$) and $n = E_{oxide}/E_f$ and $m = h_{oxide}/h_f$.

Fig. 3 shows the effect of N$_2$/O$_2$ flow ratios, R, on the residual stress and the α values. The residual stress is proportional to the elastic constant. That is, the higher the E_f value the larger the stress, compressive stress in this case. It is interesting that when the E_r (the reduced elastic modulus) values are greater than 200 GPa, tensile stress appears at low R ($= 0.5$). It is abnormal because the stress-state of all the film is compressive as observed in SEM micrographs. We believe that it is strongly affected by the E_r values and the reasonable range of E_r values will be discussed later.

Si$_3$N$_4$ and ZnS:SiO$_2$ films have been used in commercial optical disks and the reported α values were 3×10^{-6}/k and 7×10^{-6}/k [12], respectively. These α values seem to be higher than some data of TaO$_x$N$_y$ films. That is to say, if we can tune the N$_2$/O$_2$ flow ratio (R), the α values of TaO$_x$N$_y$ films can be comparable with those of Si$_3$N$_4$ and ZnS/SiO$_2$ films. Thus, TaO$_x$N$_y$ films will be superior to these two films for optical disk application in this regard.

The film stress σ_f is determined when the exact E_f can be obtained. The thin film properties may be quite different from those of bulk values and can hardly be obtainable by using current techniques used in bulk materials. Furthermore, the film properties are strongly dependent on preparation methods, processing parameters, film thickness and film compositions. Herein, we assume that the elastic constants of TaO$_x$N$_y$ films are constant, that is to say, the elastic constants are independent of their compositions. In Fig. 4 the E_r values
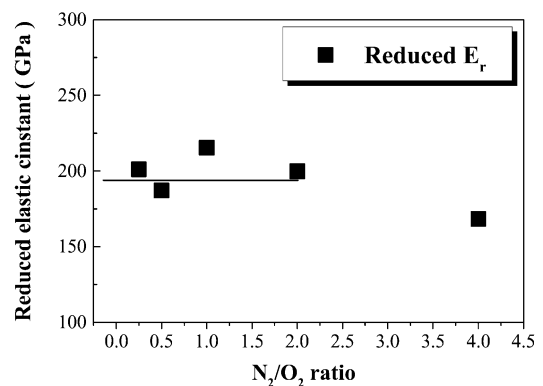

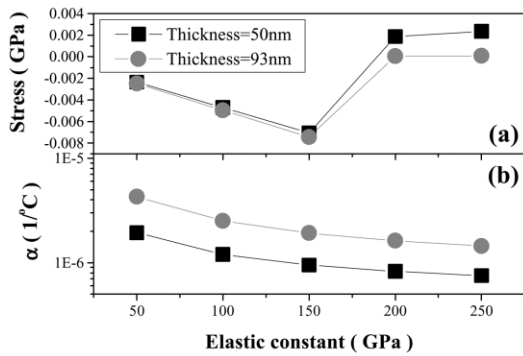Fig. 4. The reduced elastic constant (E_r) examined by nanoindentation for films deposited under variant N$_2$/O$_2$ ratios.

Fig. 5. Thickness effect on (a) residual stress and (b) α value of the TaO$_x$N$_y$ films.

were obtained by nano-indentation. According to Pharr and Oliver's formulas [13]:

$$\frac{dP}{dh} = \frac{2}{\sqrt{\pi}} E_r \sqrt{A} \tag{5}$$

$$\frac{1}{E_r} = \frac{1 - (\nu_f)^2}{E_f} + \frac{1 - (\nu_{\text{diamond}})^2}{E_{\text{diamond}}} \tag{6}$$

Here, the load (P), displacement (h) and the projected area of impression (A) are the major parameters during indentation and they are measured simultaneously. Two parameters, the film elastic modulus (E_f) and Poisson's ratio (ν_f), are required in the calculation of reduced elastic modulus (E_r). The diamond term is too small and usually can be neglected in the E_r calculation. According to the nature of Poisson's ratio, the ν_f value is usually smaller than 0.5. Thus, the film elastic modulus (E_f) would be smaller than the measured E_r values. The reduced elastic modulus (E_r) of the TaO$_x$N$_y$ films are within the range of 200 ± 15 GPa except the films deposited at R (N$_2$/O$_2$ flow ratio) of 4 (Fig. 4). That is to say, the assumption of film elastic constant below 200 GPa is reasonable.

4. Discussion

4.1. Effect of thickness on residual stress and α value of TaO$_x$N$_y$ films

In Fang et al.'s research [14], the residual stress in AlCu alloy films is affected by different thickness and altered from compressive to tensile stress state. In this study, the thickness effect on stress and the α value of TaO$_x$N$_y$ films was also investigated by using two thickness, 50 and 93 nm, that are the usual thickness of upper and bottom protective layer used in commercial optical disks, 30–50 nm and 90–130 nm, respectively. The films studied here were prepared at RF power 40 W and the N$_2$/O$_2$ flow ratio 4:1 and the (N$_2$+O$_2$)/Ar ratio 1:1, respectively. As increasing thickness the residual stress, Fig. 5a and the α value, Fig. 5b, increased as

well. Previous work [15] reported that the compressive stress originated from impurities, such as the un-reacted Ta, Ar or nitrogen gas and Ta–N clusterings that will accumulate as increasing film thickness. According to the results of the α values and residual stress values, the thicker TaO$_x$N$_y$ film is more sensitive to heating process. However, thermal behaviors can be modified by adjusting film composition (x, y values by R), so that the TaO$_x$N$_y$ films can be suitable for the application as dielectric layers of magneto–optical disks and phase-change type optical recording media.

4.2. Effect of RF power on residual stress and α value of TaO$_x$N$_y$ films

The effect of RF power (40 W, 50 W) on residual stress and the α value of TaO$_x$N$_y$ films are shown in Fig. 6. The films studied were deposited with N$_2$/O$_2$ flow ratio 4 and (N$_2$+O$_2$)/Ar ratio 1. Comparing with the film deposited at 40 W, the residual stress and the α value are smaller. During film sputtering process, the higher the power the larger is the particle energy and the deposition rate is also promoted simultaneously. The high-energy bombardment will be helpful to the film density and the compressive state by atomic peening effects. However, higher deposition rate at lower temperature (comparing with the melting temperature) would be harmful to the film density. According to the zone model for sputtered films proposed by Thornton [16], at $T_s/T_m < 0.2$, a comb-like low density region will surround the columnar microstructure and the film becomes worse as deposition rate is higher. The deposition rates at 40 W and 50 W were 1.9 and 5.5 nm/min, respectively and the surface roughness of as-deposited films examined by scanning probe microscopy (SPM) was smaller than 10 nm [15], which coincides with the characteristics of zone-1 in Thornton's model.
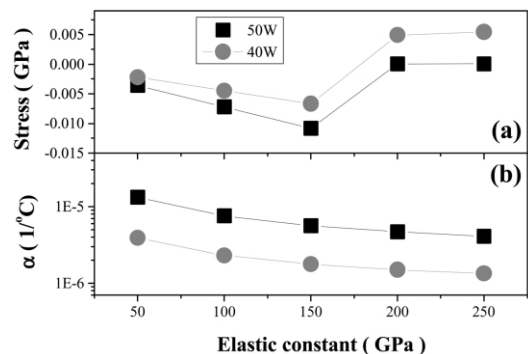

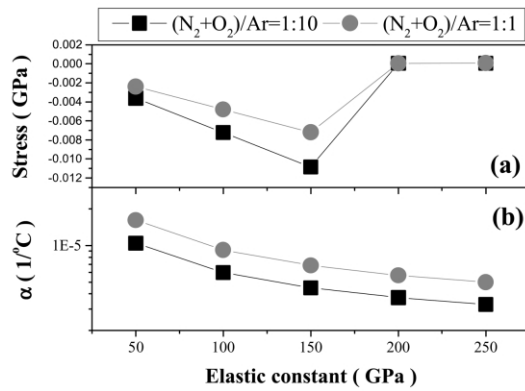Fig. 6. The RF power effect on (a) residual stress and (b) the α value of the TaO$_x$N$_y$ films.

Fig. 7. The effect of $(N_2+O_2)/Ar$ ratio on (a) residual stress and (b) the α value of TaO_xN_y films.

4.3. Effect of $(N_2+O_2)/Ar$ ratio on residual stress and α value of TaO_xN_y films

The effect of $(N_2+O_2)/Ar$ ratio on the α values (0.1 and 1) and residual stress of TaO_xN_y films was investigated and shown in Fig. 7. The films were prepared at N_2/O_2 flow ratio 1 and RF power 40 W. The deposition rate for these two conditions was 1.9 and 5.8 nm/min, respectively. Higher compressive stress and lower α value were obtained as more Ar was introduced. The refractive index (n) for films with higher Ar ratio is approximately 2.2, being higher than that with the lower Ar ratio, approximately 1.9 [15]. Since $n = C/u$, where the C and u are the velocity of light in vacuum and in the film, respectively, the higher refractive index is due to lower u that arises from a porous structure due to the higher Ar ratio. Higher Ar ratio also leads to a lower α value due to the similar reason. The columnar structure was observed for TaO_xN_y film by SEM [17]. It is therefore believed that a columnar structure is denser inside the column and looser between the columns to explain the results measured by cantilever beam.

5. Conclusions

In this study, investigation was made on some mechanical properties of as-deposited TaO_xN_y films by RF-sputtering onto SiO_2/Si and SiO_2 cantilever beam substrates by changing preparation parameters, such as the N_2/O_2 flow ratios, the $(N_2+O_2)/Ar$ ratio, RF power and film thickness. The results are summarized as follow:

1. The as-deposited TaO_xN_y films show a compressive residual stress state that increases inversely with the N_2/O_2 flow ratio and the residual stresses are within the range from 2.5 to 12.5 MPa.
2. The thermal expansion coefficient (α) values increase proportional to the N_2/O_2 flow ratio. When the films are to be used as dielectric layers for optical

recording purposes, it can be effective to reduce the stress cycling damage by tuning the α value through the N_2/O_2 flow ratio.
3. Due to the trapping of impurities and the atomic peening effect upon the film, a compressive state piles-up as the film thickness is increased and the α value is also increased.
4. Because of the combined effects of RF power and deposition rate, the film at higher power shows a lower residual stress and the α values due to lower film density.
5. The film deposited at higher Ar ratio has a structure that is denser within the column and looser between the columns.
6. Since the exact Young's modulus (E_f) value of the studied film is unknown, the residual stress and the α values were calculated under the assumption of constant E_f, independent of film compositions. The exact degree of deviation is unknown. The nanoindentation method was used to obtain the reduced elastic constant. By this method we can calculate the reduced elastic modulus E_r value $\sim 200 \pm 15$ GPa. This leads to the fact that the E_f value will be < 200 GPa and previous calculations on the α value and residual stress are reasonable.

References

[1] M.B. David, V.M. Bright, Proc. SPIE, Micromachined Devices and Component III, 3224, Austin, TX, Sept, 1997.
[2] J.W. Suh, S.F. Glander, R.B. Darling, C.W. Storment, Sens. Actuators A 58 (1997) 51–60.
[3] H.P. Trah, H. Baumann, C. Doring, H. Goebel, T. Grauer, M. Mettner, Sens. Actuators A 39 (1993) 169–176.
[4] W.K. Schomburg, R. Ahrens, W. Bacher, S. Engemann, P. Krehl, J. Martin, IEEE International Conference on Solid-State Sensors And Actuators, Chicago, June 16–19, 1997, pp. 365–368.
[5] A. Garcia, F.J. Gracia, Sens. Actuators A 46-47 (1995) 218–221.
[6] O. Atsushi, S. Kazutomi, C. Kiyoshi, US patent, #US5560998, 1 Oct. 1996.
[7] S. Masahiko, H. Kazuhiko, O. Atsushi, US patent, #US5786078, 28 July, 1998.
[8] S. Johansson, F. Ericson, J. Schweitz, J. Appl. Phys. 65 (1989) 122–128.
[9] W. Fang, H.-C. Tsai, C.-Y. Lo, Sens. Actuators 72 (1999) 22–27.
[10] F. Fasudhd, IEEE, Micro Electro Mechanical Systems Workshop, February 1990, Napa Valley, California, 1994, p. 174.
[11] S.P. Timoshenko, J. Opt. Soc. Am. 11 (1925) 233–255.

[12] H. Kitaura, T. Akiyama, T. Ohta, K. Nagata, K. Kawahara, N. Yamada, US patent, #US5681632, 28 Oct. 1998.

[13] G.M. Pharr, W.C. Oliver, J. Mater. Res. 7 (1992) 1564–1583.

[14] W. Fang, J.A. Wickert, J. Micromech. Microeng. 6 (1996) 301–309.

[15] C.-A. Jong, T.-S. Chin, 45th SPIE Annu. Proc. 4099 (2000) 246–254.

[16] J.A. Thornton, J. Vac. Sci. Technol. A4 (1986) 3059.

[17] C.-A. Jong, T.-S. Chin, Mater. Chem. Phys. In revision, (2001).